



TITLE:

Physico-chemical Studies on Surface Active Agents. (III) : The Coagulation of Sols Protected with Surface Active Agents by Inorganic Ions

AUTHOR(S):

Watanabe, Akira

CITATION:

Watanabe, Akira. Physico-chemical Studies on Surface Active Agents. (III) : The Coagulation of Sols Protected with Surface Active Agents by Inorganic Ions. Bulletin of the Institute for Chemical Research, Kyoto University 1960, 38(2-3): 216-233

ISSUE DATE:

1960-06-30

URL:

<http://hdl.handle.net/2433/75760>

RIGHT:

Physico-chemical Studies on Surface Active Agents. (III)

The Coagulation of Sols Protected with Surface Active Agents by Inorganic Ions

Akira WATANABE*

(Tachi Laboratory)

Received March 15, 1960

Studies were made on coagulation of silver iodide sols "protected" with STS by addition of various electrolytes. The stability factor obtained from turbidity measurements was a linearly decreasing function of the ratio of particle radius and double layer thickness, with a large slope for cations of high binding power. These were in good agreement with the proposed theory, in which both of the changes in the Stern potential and ionic strength were taken into account. The maximum numbers of available sites obtained from zeta potential measurements had consistently almost the same value for different counter ions. Moreover, their average value was in remarkable agreement with the number of tetradecyl sulphate ions adsorbed in the second layer on the particle surface, suggesting that the binding sites were provided by sulphate head groups in this layer. The free energies of counter ion binding were also in accord with the binding strengths between the head group and cations.

I. INTRODUCTION

Although various studies have been made on the phenomenon of counter ion binding on to surfaces of naturally occurring sol particles^{1,2)}, situations are complicated by the fact that such surfaces are usually composed of various kinds of ionogenic groupings. It has been shown in Part 2³⁾ that at fairly high surface active agent concentrations second layer adsorption starts to take place on silver iodide sol particles, and the Stern plane of this layer behaved as if it were an ideal polarised electrode. Therefore, sol particles protected with surface active agents provide ideal systems for studying this phenomenon, since various simple surfaces can be constructed which are composed of only one kind of ionic groups. Thus, we can use these systems as models for basic studies on the various phenomena which can occur at surfaces of biological importance.

One of the useful methods of obtaining basic information is to study the coagulation which occurs on addition of electrolytes. If counter ion binding takes place with such surfaces, decrease in surface potential, and under certain circumstances reversal of charge, occurs, producing a change in sol stability. However, since the free energy of counter ion binding is usually much smaller than the free energy of adsorption of surface active agents, the electrolyte must usually be added at higher normalities than the surface active agent in order to produce coagulation. Hence, a change in ionic strength also occurs, and must be taken into consideration.

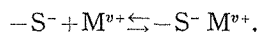
* 渡 辺 昌

The generalized theory of coagulation derived in Part 1⁴, including the case of both ϕ_s and τ changings, is therefore applicable to this problem, and an attempt has been made to test this by carrying out experiments on silver iodide sol particles protected with STS with an initial ζ value of -0.089 volt. The coagulation behaviour which occurred on addition of various electrolytes, containing different cation, at different concentration has been observed; the changes in ζ potential were also recorded.

II. THEORETICAL

1. Counter Ion Binding

Let us examine the adsorption of counter ions (cations in the present case) on the negative surface sites of protected sol particles using the usual theory of ion binding^{2,5}; it will be shown later that the negative head groups of the second layer will probably provide the adsorption sites for the counter ions. As the experimental data suggest that the maximum number of available sites in the second layer is very small, *vide* also Part 2³, the problem can be treated as a case of ion binding on N_2 independent sites. For this system the reversible association-dissociation equilibrium applies, *viz.*



where $-S^-$ is the negatively charged surface site and M^{v+} the v -valent counter cation. If the number of ions bound is n_2 and the molar concentration of counter ions in the bulk phase is c_e , we obtain for this equilibrium,

$$\frac{n_2}{(N_2 - n_2) c_e} = k_2^p \quad (1)$$

where k_2^p is the equilibrium constant of the surface reaction.

Equation (1) can easily be transformed to:-

$$n_2 = \frac{N_2 k_2^p c_e}{1 + k_2^p c_e} \quad (2)$$

The constant k_2^p is similar to the adsorption constant in equation (44) of Part 1 in the sense that it is dependent on the surface potential and related to the electrochemical free energy of binding, $\Delta \bar{G}$, by

$$k_2^p = \exp(-\Delta \bar{G}/kT)/55.6 \quad (3)$$

vide equation (45) of Part 1. At the same time, similar equations for ϕ_s potential behaviour can be used as in Part 1. However, it must be taken into account that the ionic strength, and hence τ , can change rapidly in the present case. The equations which can be obtained from these considerations are as follows, *vide* equation (69) of Part 1:

$$\phi_s - \phi_s^p = \Delta \phi_s = -\frac{\theta N_2 v k_2^p c_e}{(1 + k_2^p c_e)(1 + \tau)} \quad (4)$$

$$\text{where } \theta = 4 \pi a e / \epsilon \quad (5)$$

and

$$\frac{d \phi_s}{d \ln c_e} = \Delta \phi_s \left[1 - \frac{k_2^p (1 + \tau)}{\theta N_2 v k_2^p} \right] \quad (6)$$

Here ϕ_s^p is the value of ϕ_s for the protected sol particles, *i.e.* for the second adsorption layer, instead of the ϕ_s of the first layer.

2. Application of the Generalized Theory of Coagulation

Equation (72) of Part 1 is complicated and not very convenient for obtaining a general picture of the stability behaviour; its application will therefore be restricted to special cases, where a direct comparison can be made with experimental results. In the following an assumption will be made such that ϕ_s is the potential which is effective in the coagulation process, *vide* Part 1 and 2.

(i) The Slope of the $\ln W$ vs. τ Curves in the Absence of Ion Binding

The general equation (72) of Part 1 becomes very simple in this case, since if $k_2^p \rightarrow 0$, *i.e.* no ion binding, we obtain for an arbitrary c_e ,

$$\frac{d \ln W}{d \tau} \rightarrow - \frac{\varepsilon a (\phi_s^p)^2 u_m \exp(-\sqrt{p} u_m)}{kT (u_m + 2)} \quad (7)$$

For conditions of $\phi_s^p = 90$ mV, $a = 100$ Å, and $p = 1$ (*i.e.* the ionic strength of $10^{-3}M$), the calculated slope is -5.53 , if u_m is assumed to be 0.07 , *vide* Part 1. Moreover, in the absence of ion binding for conditions such that $u_m \sqrt{p} \ll 1$, we may write

$$\frac{d \ln W}{d \tau} \rightarrow - \frac{\varepsilon a (\phi_s^p)^2 u_m}{kT (u_m + 2)} \quad (8)$$

As it has been shown in Part 1 that the value of u_m does not change very much with τ , it can be concluded that $\ln W$ is a linearly decreasing function of τ .

(ii) The Initial Slope of $\ln W$ vs. τ Curves

For an arbitrary value of k_2^p , the initial slope of the $\ln W$ vs. τ curves for increasing electrolyte concentration is obtained from equation (72) of Part 1 by taking $c_e \rightarrow 0$, *i.e.* $\tau^2 \rightarrow p$, as

$$\frac{d \ln W}{d \tau} = \frac{-\varepsilon a \exp(-\sqrt{p} u_m) \phi_s^p}{kT (u_m + 2)} \left[\phi_s^p u_m + \frac{4 \theta N_2 v k_2^p \sqrt{p}}{(1 + \sqrt{p}) q} \right] \quad (9)$$

Since both the Stern potential of the particles and the ionic strength are constant for a given protected sol, ϕ_s^p and p are constant. We can therefore conclude from equation (9) that the higher the values of N_2 and k_2^p , the larger will be the initial slope of the $\ln W$ vs. τ curve. The valency of the counter ion enters into numerator and also to denominator *via* q , so that its effect is not immediately apparent. Especially for a large value of k_2^p , *i.e.* for strong counter ion binding, $-d \ln W / d \tau$ will become very large and tend to infinity; this corresponds to the case of coagulation caused by the change in surface potential, *vide* Part 2.

All of the $\ln W$ vs. τ curves start from the value of $\ln W$ corresponding to the original protected sol, *i.e.* at the initial ionic strength.

III. EXPERIMENTAL

1. Materials

The anionic surface active agent used was STS and of the same quality as in

Part 2. All inorganic salts used as coagulating agents were of Analar grade. In the case of calcium nitrate, a 1.5 M solution was prepared by adding the calculated amount of conc. nitric acid to a known amount of calcium carbonate.

2. Preparation of Protected Sols

The positive silver iodide sol was prepared in the manner described in Part 2, except that all concentrations were doubled. The sol prepared, therefore, had a concentration of $10^{-3} M$, an ionic strength of $3 \times 10^{-3} M$ and contained $10^{-3} M$ potassium nitrate and $2 \times 10^{-3} M$ silver nitrate.

3 ml of $2 \times 10^{-4} M$ STS were added to an equal volume of the above sol in a Pyrex test tube, to obtain a negatively charged sol protected with STS. The final concentrations were, therefore, exactly the same as in the case of Part 2, except that they contained in addition $10^{-4} M$ STS. This preparation was performed for each experiment 5 min before use. The value of ζ potential for particles of this sol was -89 mV ; this was in the range of stabilized sol, see Fig. 16 of Part 2.

3. Methods of Measurements

(i) Turbidity

Aliquots of salt solutions were added by the mixing device to 3 ml of the protected silver iodide sols in the optical cell and the turbidity change with time was followed by the method previously described³⁾.

In the case of lithium nitrate, the coagulation reaction was very slow compared with the case of other coagulating electrolytes. The turbidity change with time was therefore observed directly 1, 2 and 10 min after mixing.

(ii) Microelectrophoresis

Aliquots of electrolyte solutions were added with vigorous stirring to 6 ml of protected silver iodide sols in Pyrex test tubes, and the mobilities of the sol particles were measured by ultra-microelectrophoresis. The experimental determination and calculation of ζ potential were the same as those described in Part 2.

IV. RESULTS

1. Measurement of Stability by Turbidimetry

(i) Optical Density *vs.* Time Curves

The changes in turbidity of the protected sols which occurred on the addition of inorganic electrolytes were typical of coagulation processes. As an example the optical density *vs.* time curves for the case of addition of manganese sulphate are shown in Fig. 1. The early portions of the curves were sufficiently linear to enable the initial slope to be obtained, and hence the stability factor, W .

In the same figure the optical density change caused by the addition of manganese sulphate to a positive silver iodide sol not protected with STS is shown. On comparing this with the corresponding curve for the protected sol, at the same salt concentration ($5 \times 10^{-3} M$), it is clear that protection by STS is taking place; it is the sulphate ion which causes coagulation of the positive sol, and the manganese

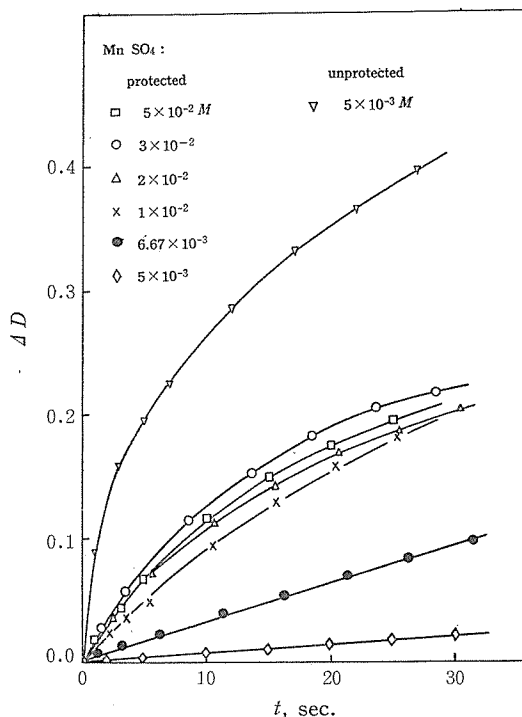


Fig. 1. Δ Optical density *vs.* time for coagulation of Ag I sol, protected with $10^{-4} M$ STS, by $MnSO_4$. A curve is also shown for the coagulation of an unprotected sol.

ion which coagulates the protected sol, *cf.* Table 1 of Part 2. It has also been confirmed that the unprotected sol was not coagulated by addition of $1.8 \times 10^{-2} M$ barium nitrate, whilst the protected sol at this concentration of barium nitrate showed coagulation. These facts are sufficient to show that in the former case the anionic species is chiefly effective in causing coagulation and in the latter case the cationic species.

(ii) $\log W$ *vs.* $\log c_e$ Curves

The stability factor, W , was calculated from the initial slope of the optical density, D , *vs.* time; t , curves by using equation (14) of Part 1, *viz.*

$$\log W = \log (dt/dD) - 1.46 \quad (10)$$

The value of the initial slope was usually obtained in the same manner as in Part 2. However in the case of lithium nitrate, it was obtained from the increase in optical density over the first 1 min interval, see previously.

The $\log W$ *vs.* $\log c_e$ curves in Fig. 2 thus obtained clearly show the rapid and slow coagulation ranges. Although they are very similar to the curves obtained by Reerink and Overbeek¹⁰, their theory cannot be applied directly, since both ionic strength and surface potential are changing with salt concentration in the present system.

Although almost all of the curves have a very similar shape with almost the same slope in the slow coagulation range, thorium and calcium ions give different

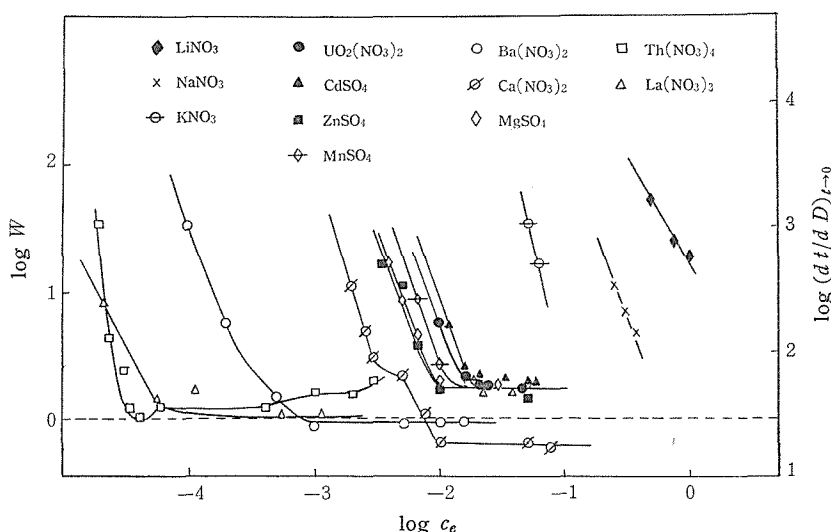


Fig. 2. Log stability factor *vs.* log molar concn. of added electrolytes. Ag I sols protected with STS.

type of curves. It is clear from a comparison with the results obtained in Part 2, that the behaviour of the thorium ion is very much similar to that of the citrate ion against the positive silver iodide sol. This indicates that with increasing concentration the extremely high valency of the thorium ion gives rise to a large change in the ψ_s value by binding with the surface and moreover changes the sign of surface charge. Hence, the same mechanism of coagulation appears to hold as described in Part 2 for coagulation produced by the binding of highly charged counter ions; coagulation is caused primarily by the change in ψ_s . In addition to this mechanism the ionic strength change must also be taken into account at higher concentrations; it is noticed on the same curve in the high concentration range that, as expected, the stability factor does not acquire a high value.

The lanthanum ion appears to show the usual type of curve for coagulation due to increasing ionic strength and no reversal of charge has been observed, see Fig. 3. However, the barium and calcium ions show some peculiarities, since for both ions values of W lower than unity are obtained at higher concentration.

2. Measurement of ζ Potential by Electrophoresis

In Fig. 3 ζ *vs.* $\log c_e$ curves for various coagulating agents are shown. It can be concluded from these curves that in most cases changes in ζ potential is taking place and must be taken into account in discussing the coagulation phenomena by these ions. However, in the case of ions of the alkali metals, the ζ potential remains virtually constant over the concentration range investigated, indicating that little adsorption is taking place for such low valent ions; this is similar to the situation observed by the mercury electrode, where little binding of potassium, sodium and lithium ions *etc.*, occurs.

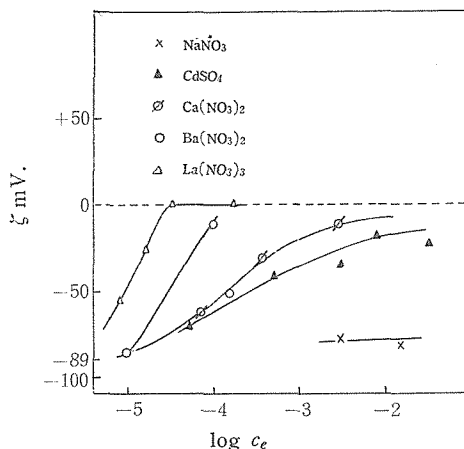


Fig. 3. ζ vs. log molar concn. of added electrolytes.
Ag I sols protected with STS. $\zeta^p = -89$ mV

V. DISCUSSION

1. Turbidity Behaviour

(i) Precipitation Reactions between Ionic Species in the Bulk

All the coagulating agents were used in the forms of nitrates or sulphates, and the sols contained 10^{-3} M silver ions.

As the solubility of silver nitrate is very high, precipitation of silver nitrate is unlikely to take place in the present case.

The solubility product of silver sulphate has been calculated as 3.2×10^{-5} from the solubility value of 2×10^{-2} M at room temperature, assuming complete dissociation. This means that in the presence of 10^{-3} M silver ion no precipitation of silver sulphate will occur until the sulphate ion concentration becomes larger than 32 M.

The reaction between the silver ion and the tetradecyl sulphate ion has been found, by turbidity measurements, to give no precipitation under the condition used, *i. e.* $[\text{Ag}^+] = 10^{-3}$ M and $[\text{STS}] < 10^{-4}$ M.

It can be concluded, therefore, that the reactions between the silver ion and various anions, including the tetradecyl sulphate ion, do not interfere with the turbidity measurements under the conditions used. However, reactions between the tetradecyl sulphate ion and the various cations added as coagulating agents could occasionally cause interference. In Table 1 the solubility products of various insoluble salts are shown; they have been calculated from the experimental data presented in Part 5⁷. In the same table are given the calculated values of the maximum permissible concentrations of corresponding cations which can be added without causing precipitation for an STS concentration of 10^{-4} M. The stoichiometric concentration of STS in the sol is taken as 10^{-4} M, *i. e.* as if there were no decrease in the bulk concentration due to adsorption. However, in practice the bulk concentration of STS in the sols is always less than 10^{-4} M, although the difference may be small at such a comparatively high STS concentration.

It is clear from the values in this table that the turbidity changes, and hence the stability factors, are generally not interfered with by the formation of the corresponding tetradecyl sulphate salts in the ranges of major interest. The only exceptions occur in the case of barium and calcium ions. It is clear from the values in the third column of Table 1, that precipitation starts to take place in the range where the stability factor is changing, or at least very near to it. This suggests that the values of $\log W$ lower than unity, which were found for the rapid coagulation ranges for these ions (*vide* Fig. 2), will probably be due to the extra increases in optical density resulting from the precipitation of corresponding tetradecyl sulphate salts, *i. e.* larger number of particles formed.

Table 1. Solubilities of tetradecyl sulphate salts.

Salt**	Solubility product <i>M</i> /litre	Cation concentration for $[\text{TS}^-]=10^{-4}M$ <i>M</i> /litre	Solubility <i>M</i> /litre
Th(TS) ₄ ***	2.0×10^{-17}	2.0×10^{-1}	1.5×10^{-4}
La(TS) ₃	4.0×10^{-14}	4.0×10^{-2}	2.0×10^{-4}
Ba(TS) ₂	2.0×10^{-11}	2.0×10^{-3}	1.7×10^{-4}
Ca(TS) ₂	2.5×10^{-11}	2.5×10^{-3}	1.8×10^{-4}

** Mg, Zn, Mn, Cd, UO₂, K, Na and Li salts are soluble.

*** TS⁻ = tetradecyl sulphate ion.

(ii) Coagulation Concentration

In the same manner as described in Part 2 the coagulation concentrations of various salts for the protected silver iodide sols can be obtained by extrapolating the linear portions of the $\log W$ *vs.* $\log c_e$ curves to $\log W=0$. It is of interest to compare the values thus obtained with the coagulation concentration of sols of the corresponding tetradecyl sulphate salts, *vide* Table 2. The latter values were obtained by extrapolating the steeply increasing portions of the optical density *vs.* $\log c_e$ curves, which were obtained by adding electrolyte solutions of various concentrations to a $10^{-3} M$ STS solution, to the $\log c_e$ axis, *vide* Part 5⁷. It has been checked by electron microscopy, as well as by direct observation using the ultramicroscope, that the very steep increase in turbidity at certain electrolyte concentrations was due to coagulation of the sols formed.

Comparison of these two sets of coagulation concentrations shows a marked parallelism; this becomes much clearer if a, so-called, cation coagulation spectrum for silver iodide sols protected with STS is constructed, see Fig. 4. It is noticed that the various cations give the same sequence independent of whether they are used to coagulate sols protected with STS or to coagulate sols of the corresponding tetradecyl sulphate salts. This fact appears to indicate that the surface of a protected sol has essentially the property of the head group of the anionic surface active agent and the coagulation problem can be treated by considering only the Stern plane of the second layer.

In this connexion it is worth while to consider whether the sulphate head groups of STS in the second adsorption layer are directed towards the solution or away

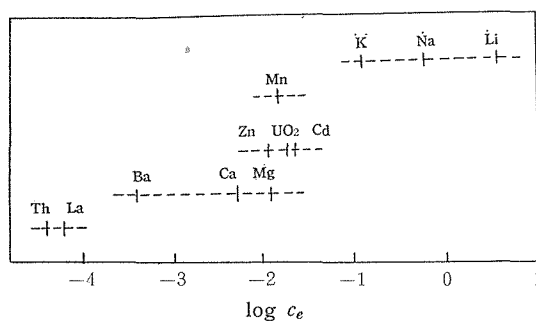


Fig. 4. Cation coagulation spectrum for Ag I sols protected with STS.

from it. The following consideration seems to suggest strongly that the former is more likely to be the case under the circumstances considered here. When the coagulation concentrations of the various electrolytes for protected sols in Table 2 are compared with the solubilities of the corresponding tetradecyl sulphate salts in Table 1, we again find that the same cationic sequence is obtained; the only exception is the position of lanthanum, which can be explained on the basis of the free energy of binding, see later (Table 4). It is concluded therefore that the lower the solubility of the corresponding salt the lower will be the coagulation concentration for a protected sol. This shows that the adsorption mechanism of a cationic species on to the protected surface is intimately related to the bond strength between the cation and the sulphate head group of the surface active agent. In other words, the sulphate groups are more likely to direct themselves towards the solution in the case of second layer adsorption.

A relation between the adsorbability and the solubility has also been found in experiments using the mercury electrode. For example, in the case of a positively charged mercury surface, the adsorbability of an anion is highest for an anion which

Table 2. Coagulation concentrations of various electrolytes for the silver iodide sols protected with $10^{-4}M$ STS and for the sols of the corresponding tetradecyl sulphate salts.

Electrolyte	Coagulation concentration for the sol protected with STS M/litre	Coagulation concentration for the sol of the TS salt M/litre
Th(NO ₃) ₄	3.98×10^{-5}	1.9×10^{-4}
La(NO ₃) ₃	6.16×10^{-5}	2.0×10^{-4}
Ba(NO ₃) ₂	3.80×10^{-4}	2.4×10^{-3}
Ca(NO ₃) ₂	4.90×10^{-3}	2.9×10^{-3}
MgSO ₄	1.18×10^{-2}	soluble
ZnSO ₄	1.18×10^{-2}	soluble
MnSO ₄	1.45×10^{-2}	soluble
UO ₂ (NO ₃) ₂	1.91×10^{-2}	soluble
CdSO ₄	2.24×10^{-2}	soluble
KNO ₃	1.20×10^{-1}	soluble
NaNO ₃	5.75×10^{-1}	soluble
LiNO ₃	3.72	soluble

forms the most insoluble mercury salt^{8,9}. Grahame explained this highly specific adsorption by assuming that the interaction between the mercury surface and the anion is not only electrostatic but resembles chemical bonding. This seems to hold also in the present case; most of the cations used in the present experiments are possibly somewhat dehydrated on adsorption to the sulphate sites and the linkage is probably more akin to a chemical bond.

2. Adsorption Behaviour of the Counter Ions

(i) Maximum Number of Available Sites for Counter Ion Binding

In Table 3 values of N_2 calculated by using equation (6) are listed. In this calculation the slopes of the ζ vs. $\log c_e$ curves at an arbitrarily chosen $\Delta\zeta$ value of 0.05 volt were used, since the reversal of charge did not always occur. It is noticed that the values of N_2 are in remarkably good agreement with each other in spite of the fact that the cationic species have very different properties. The average value of N_2 obtained is $4.23 \times 10^{13} \text{ cm}^{-2}$ and the area occupied by a counter ion at maximum coverage is $2360 \pm 500 \text{ \AA}^2$.

In the last section an experimental fact has been shown which strongly suggests that the head groups of STS in the second adsorption layer are directed towards the solution phase and provide the sites for counter ion binding. Another fact which appears to support this statement is given by comparing the above value of N_2 with the number of head groups in the second layer.

Table 3. Parameters of counter ion binding for a silver iodide sol protected with $10^{-4} M$ STS. $a=100 \text{ \AA}$, $\Delta\zeta=0.05$ volt

Counter ion	Concentration** M/litre	τ	$d\zeta/d \log c_e$ volt	$N_2 \text{ cm}^{-2}$
La ⁺⁺⁺⁺	1.20×10^{-5}	1.25	6.0×10^{-2}	3.45×10^{12}
Ba ⁺⁺⁺	4.36×10^{-5}	1.28	6.0×10^{-2}	5.25×10^{12}
Ca ⁺⁺	2.63×10^{-4}	1.51	4.0×10^{-2}	4.24×10^{12}
Cd ⁺⁺	6.60×10^{-4}	1.87	2.3×10^{-2}	3.96×10^{12}
Average				4.23×10^{12}

** Concentration of the added electrolyte giving $\Delta\zeta$ value of 0.05 volt.

If the numbers of surface active agents adsorbed in the first and second layer on a silver iodide sol particle are n and n' per cm^2 respectively, equation (19) of Part 2 can be rewritten as

$$n + n' = \frac{N_1 k_2 c}{1 + k_2 c} + \frac{N_1' k_2' c}{1 + k_2' c} = \frac{\varepsilon(1 + \tau)}{4 \pi a e} (\zeta^* - \zeta) \quad (11)$$

where c is the surface active agent concentration in M , N_1 and N_1' are the maximum numbers of available sites and k_2 and k_2' are the adsorption constants of the first and second adsorption layers of the surface active agent. Now, we have obtained the values of N_1 and k_2 for STS, *i.e.* $1.94 \times 10^{13} \text{ cm}^{-2}$ and $1.61 \times 10^5 \text{ litre}/M$ respectively, *vide* Table 3 of Part 2. Hence, substituting the experimental values of

$\zeta = -0.089$ volt for $c = 10^{-4} M$ in equation (11) together with $\tau = 1.23$ and $\zeta^* = 0.140$ volt, we obtain

$$n' = 4.5 \times 10^{12} \text{ cm}^{-2}$$

This value is in excellent agreement with the average value of N_2 obtained above, *i. e.* $4.23 \times 10^{12} \text{ cm}^{-2}$. This fact also suggests that the sites for counter ion binding of the protected sol particles are very probably only the head groups of the surface active agents adsorbed in the second layer.

(ii) Free Energy of Counter Ion Binding

In Table 4 the values of k_2^p , $\Delta \bar{G}$ and ΔG for the various cationic species are given. These were obtained from equations (4) and (3) by substituting $N_2 = 4.23 \times 10^{12} \text{ cm}^{-2}$, $\Delta \zeta = 0.05$ volt and the values of τ and c_e of Table 3. When these values of ΔG are compared with the free energy of adsorption of STS, *i. e.* $-9,410$ and $5,655$ cal/mole (*vide* Part 2) for the first and second layer respectively, it is found that the binding energy of counter ions is of the same order of magnitude as the second layer adsorption of STS. Moreover, the values are of the order of magnitude expected for counter ion binding²⁹.

Table 4. Free energy of counter ion binding on the silver iodide sol protected with $10^{-4} M$ STS.

Cation	k_2^p litre/ M	$-\Delta \bar{G}$ cal/mole	$-\Delta G^{**}$ cal/mole
La ⁺⁺⁺	5.38×10^4	8,730	5,880
Ba ⁺⁺	3.36×10^4	8,450	5,650
Ca ⁺⁺	7.14×10^3	7,560	5,730
Cd ⁺⁺	4.59×10^3	7,350	5,520

$$^{**} \Delta \bar{G} = (-v e \zeta / kT) + \Delta G = 915 v + \Delta G$$

for $\zeta = -0.039$ volt (or $\Delta \zeta = 0.050$ volt).

It is of interest to compare the quantity $-\Delta G$ with the solubility of the corresponding tetradecyl sulphate salt as listed in Table 1. It is found that the higher the solubility of the corresponding salt, the lower is the value of $-\Delta G$; this is in accord with the conclusion obtained from an independent method, *i. e.* the stability behaviour of protected sols in the presence of counter ions, see previously.

It appears that the lanthanum ion gives an exception, since the value of $-\Delta G$ is a little larger than expected from solubility data. However, according to the thermodynamic consideration of Guggenheim¹⁰, it is impossible to divide $\Delta \bar{G}$ into an electrical and a chemical terms and hence values of $-\Delta G$ in Table 4 give only an approximate estimate of the specific binding free energy of each ion. In other words, we can compare only the ions of the same valency type by this method.

It has been observed in this connexion that the adsorption of anions on to the positively charged mercury electrode as a function of the surface charge density is more than expected from the increase in the Coulombic attraction between them. This means that the chemical free energy of adsorption is not constant but increases

with the positive charge of the mercury surface. This is also related to the fact that the positive cationic charge enhances the strength of the covalent bonding of simple inorganic salts; for instance ferrous chloride dissociates much more than ferric chloride²⁹.

In the same manner the chemical free energy of binding between a lanthanum ion and a sulphate head group is increased by the extra positive charge of the lanthanum ion over that of the univalent sulphate group, compared with the precipitation of $\text{La}(\text{TS})_3$ from which the solubility data was worked out; in the latter case the charge of the lanthanum ion will probably be neutralized by three sulphate groups.

This effect of an extra positive charge on bond strength will also exist in the case of the divalent cations, although to a lesser degree. Hence, the values of $-\Delta G$ in Table 4 are probably greater than those of the "true" chemical free energy, since this would be obtained only for a charge free case.

3. Stability Behaviour

(i) Log W vs. ζ Curves

It would be expected that the stability factor of this system would follow the same type of behaviour as described in Part 2, if the coagulation were caused only by a decrease in the surface potential due to counter ion binding.

In order to examine this hypothesis, $\log W$ was plotted against ζ in Fig. 5 for some typical cases. Although with cadmium sulphate and calcium nitrate the behaviour is almost the same as in the case of Part 2, quite a different type of coagulation is obtained with lanthanum nitrate and barium nitrate. Hence, the change in ionic strength must also be taken into account in the latter cases.

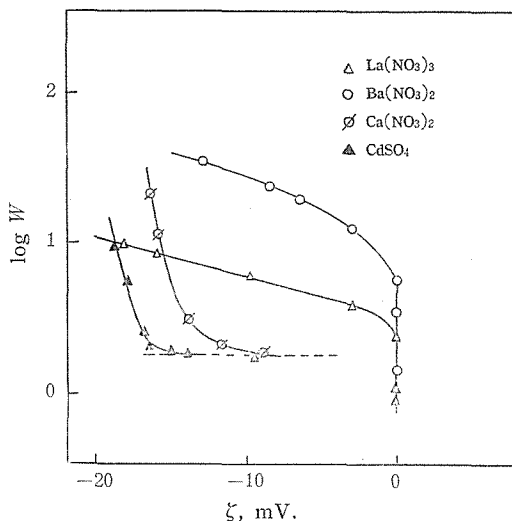


Fig. 5 Log stability factor vs. ζ .
AgI sols protected with STS.

(ii) Log W vs. τ Curves

The effect of ionic strength becomes much clearer on consideration of the \log

W vs. τ curves in Fig. 6, *vide* Part 1. They clearly indicate that coagulation by thorium, lanthanum or barium ions is mainly due to a change in surface potential in the slow coagulation range. Although a small change in τ is occurring very near to the stability minimum, in the initial region where the stability is decreasing very rapidly, the ionic strength is reasonably constant and we can assume $\tau=1.23$.

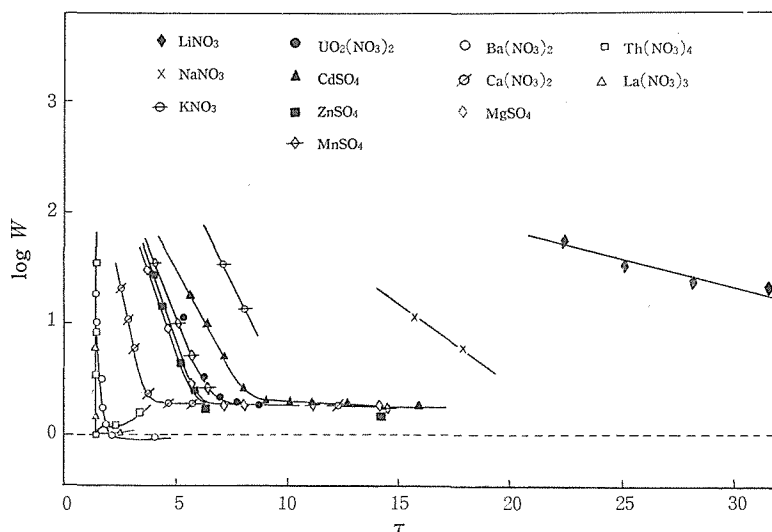


Fig. 6. Log stability factor vs. τ . Ag I sols protected with STS.

The other curves are very different from those described above in the sense that the stability change occurs with increasing τ , and moreover the $\log W$ value is a linearly decreasing function of τ . This is quite in accord with the theory derived earlier, *vide* equation (7).

Equation (9) is also satisfied by the results obtained. In the present case, N_2 is the same for all ionic species, *vide* Table 3, and v and k_2^p are different from each other. As the ζ^p value is constant, *i.e.* -0.089 volt, all quantities are the same in this equation except the last two, *i.e.* v and k_2^p . All the $\log W$ vs. τ curves should, therefore, start from the value of $\log W$ of the original protected sol with different initial slopes; the slope is larger in absolute magnitude for larger values of k_2^p , and in the case of extremely large values of k_2^p , *e.g.* the lanthanum ion, the slope is tending to minus infinity. All of these theoretical expectations are satisfied by the experimental $\log W$ vs. τ curves in Fig. 6.

(iii) Stability Minimum

The condition of the stability minimum is obtained when

$$d \ln W / d \tau = 0.$$

It is found from equation (71) of Part 1 that this is fulfilled by one of the two cases:-

$$\psi = 0 \quad (12)$$

$$\text{or} \quad \tau u_m \gg 1, \text{ i.e. } \exp(-\tau u_m) \rightarrow 0 \quad (13)$$

Equation (12) corresponds to the rapid coagulation discussed in Part 2 and in the

present case occurs only for the counter ion having large values of k_2'' and v , *e. g.* lanthanum ion. On the other hand, equation (13) corresponds to the Reerink-Overbeek mechanism of coagulation⁶⁹ and, instead of having a minimum, the value of $\log W$ tends to a limit, corresponding to rapid coagulation, with increasing τ .

The values of W for both cases, W^r , will be the same and have the following value, *cf.* equation (27) of Part 1:

$$W^r = 2 \int_0^{\infty} \exp(-A/12 u kT) \frac{du}{(u+2)^2} \quad (14)$$

This condition is a theoretical concept, but is never met with experimentally. Reerink and Overbeek⁶⁹ have avoided this difficulty in discussing their experimental results by assuming $W^r=1$ for rapid coagulation, and calculating the values of W in the slow coagulation range using this procedure. Although the expression used for $V(u)$ in equation (26) of Part 1 is different from that used by them, we can also follow the same procedure; in fact, the arguments in this paper as well as those in Part 2 are entirely based on this assumption.

The value of unity for W is obtained by the following condition, which is different from that given by equation (12) or by equation (13), *viz.*

$$V(u) = \frac{\epsilon a \psi^2}{u+2} \exp(-\tau u) - \frac{A}{12 u} = 0 \quad (15)$$

in equation (26) of Part 1. This corresponds to free diffusion in the absence of a field of force, *cf.* Part 1. However, again this condition is never satisfied mathematically, because equation (15) has no solution except when $u=\infty$. It is not possible physically either, because we can always expect the existence of van der Waals type of forces between particles, and hence completely free diffusion cannot be expected in the immediate neighbourhood of the particle surfaces.

One of the experimental facts which appears to give some idea about this problem is that, even in the "supposed" rapid coagulation range for protected sols, W is much higher than unity in the case of divalent ions, *vide* Fig. 5 and 6. This deviation of W from unity is smaller for ions having higher valency, or higher binding power; in the latter case the value of ψ becomes practically zero for rapid coagulation. This means that, the remaining potential barrier, which prevents rapid coagulation, is higher for the case of changing τ than for the case of changing ψ , *vide* Appendix.

The author takes pleasure in expressing his gratitude to Dr. R.H. Ottewill, University of Cambridge, for his kind supervision and continuous advice during the course of this work. Thanks are also due to the British Council for the Scholarship and to the University of Cambridge for the award of the Oliver Gatty Studentship. Thanks are also due to Imperial Chemical Industries, Dyestuffs Division, for supplying the STS. The author wishes also to express his gratitude to Professor I. Tachi and to Dr. S. Ueda for their continuous interest and encouragement.

APPENDIX

THE DIFFUSION PROCESS WITH A POTENTIAL BARRIER

(i) The Residual Potential Barrier in the Case of Rapid Coagulation

The concept of a potential barrier can be introduced by constructing the potential energy curve, as is schematically shown in Fig. A. 1, *cf.* Fig. 1 of Part 1. It is clear from this curve that when one particle approaches the surface of another particle (taken to be at O in the figure) the particle must have a free energy of activation, ΔF^\ddagger , before it can coalesce. This potential barrier does not reduce to zero, even if the maximum value of V , V_m , is zero; that is, although this corresponds to the case of free diffusion macroscopically, it is no longer free diffusion when the problem is considered microscopically.

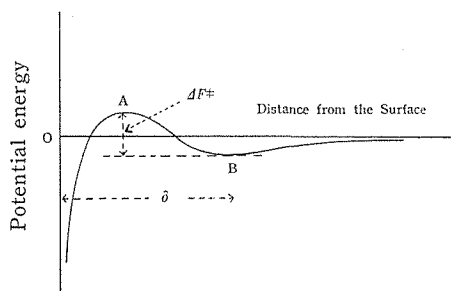


Fig. A. 1. Potential energy diagram of two approaching particles.

The particle at position B is in a meta-stable state; if the kinetic energy of translation is large enough to overcome the barrier, it can come to position O, which is a stable state with the lowest potential energy. This is a typical example of an irreversible process, and we can apply the Eyring treatment¹¹⁾, giving a relation of the form:-

$$k^\ddagger = k_f \exp(-\Delta F^\ddagger/kT) \quad (\text{A. 1})$$

where k^\ddagger is the heterogeneous reaction rate constant and k_f the frequency factor.

The change in τ has more effect on the shape of the potential energy curve, and hence on the depth of the potential minimum at B, than the change in ψ . This is due to the fact that τ appears in the equation of V_R in the form $\exp(-\tau u)$, while ψ is in the form of ψ^2 , *vide* equation (25) of Part 1.

This is quite in accord with the experimental results obtained in the text. It was found that, even in the "supposed" rapid coagulation range for protected sols, the values of W_{min} were usually higher than unity. This tendency was higher in the case of ordinary divalent cations, *e.g.* Zn^{++} , Cd^{++} *etc.*, than in the case of cations with high valency, *e.g.* Th^{++++} , or high binding strength, *e.g.* Ca^{++} , Ba^{++} *etc.*, see Fig. 6; the coagulation takes place by increase in τ in the former case and by the decrease in ψ in the latter. Hence, a deeper potential minimum at B is supposed to exist in the former case than in the latter.

(ii) Derivation of the Stability Factor, W

Another expression for W can be derived by the use of the model adopted here, leading to an equation relating W to the potential energy barrier, ΔF^\ddagger .

For the sake of simplicity, the particles are assumed to be in free diffusion until they arrive at the position B, with the coordinate δ ; at this point an irreversible reaction occurs with a rate constant k^δ .

The basic equation for the diffusion process is given by Fick's second law, *viz.*

$$\partial N / \partial t = \text{div} (\mathcal{D}' \text{ grad } N) \quad (\text{A. 2})$$

where the symbols have the same meaning as in Part 1, *vide* equation (10) of Part 1. The reaction rate is defined by

$$-\partial N(r, t) / \partial t = k^\delta N(r, t) \quad \text{for } r = \delta.$$

From Fick's first law, we have

$$-\partial N / \partial t = \mathcal{D}' (\partial N / \partial r)_{r=\delta}$$

Therefore, by combining the two equations we obtain one of the boundary conditions for solving equation (A. 2), *viz.*

$$\mathcal{D}' [\partial N(r, t) / \partial r]_{r=\delta} = k^\delta N(r, t) \quad \text{for } r = \delta \quad (\text{A. 3})$$

The other boundary and the initial conditions are respectively given by

$$N(r, t) = N_b \quad \text{for } r \rightarrow \infty \quad (\text{A. 4})$$

$$\text{and } N(r, 0) = N_b \quad \text{for } t = 0 \quad (\text{A. 5})$$

In the case of spherical symmetry, equation (A. 2) has the form:

$$\partial N / \partial t = \mathcal{D}' [\partial^2 N / \partial r^2 + (2/r)(\partial N / \partial r)] \quad (\text{A. 6})$$

The solution of this equation under the conditions given by equations (A. 3), (A. 4) and (A. 5) can be obtained by the usual methods¹²⁾, giving

$$N = N_b \left[1 - \frac{h \delta^2}{r(1 + \delta \cdot h)} \left\{ \text{erfc} \left(\frac{r - \delta}{2 \sqrt{\mathcal{D}' t}} \right) - \exp [h' (r - \delta) + h' \mathcal{D}' t] \text{erfc} \left(\frac{r - \delta}{2 \sqrt{\mathcal{D}' t}} + h' \sqrt{h t} \right) \right\} \right] \quad (\text{A. 7})$$

$$\text{where } h = k^\delta / \mathcal{D}' \quad (\text{A. 8})$$

$$\text{and } h' = h + (1/\delta) \quad (\text{A. 9})$$

This equation has already been derived by Collins and Kimball¹³⁾ from a slightly different point of view.

The coagulation rate is proportional to the flux, j , at the surface δ , *vide* Part 1, which is obtained from equation (A. 7) as,

$$j = \mathcal{D}' (\partial N / \partial r)_{r=\delta} = \frac{\mathcal{D}' N_b h}{1 + \delta \cdot h} \{ 1 + \delta \cdot h \exp (h'^2 \mathcal{D}' t) \text{erfc} (h' \sqrt{\mathcal{D}' t}) \} \quad (\text{A. 10})$$

Rapid coagulation is defined by the condition

$$\delta \cdot h' = \delta \cdot h + 1 \gg 1, \text{ i. e. } k^\delta \gg \mathcal{D}' / \delta \quad (\text{A. 11})$$

and thus we obtain the flux j^r using equation (A. 10), as

$$j^* = -\frac{\mathcal{D}' N_b}{\delta} \left(1 + \frac{\delta}{\sqrt{\pi \mathcal{D}' t}} \right) \quad (\text{A. 12})$$

Here, the series expansion of the error function complement has been used, as

$$\begin{aligned} \operatorname{erfc}(\lambda) = & \frac{\exp(-\lambda^2)}{\sqrt{\pi} \lambda} \left\{ 1 - \frac{1}{2\lambda^2} \right. \\ & \left. + \frac{1 \cdot 3}{(2\lambda^2)^2} - \frac{1 \cdot 3 \cdot 5}{(2\lambda^2)^3} \cdots \right\} \quad \text{for } \lambda > 1 \end{aligned} \quad (\text{A. 13})$$

Equation (A. 12) corresponds to the Smoluchowski equation for rapid coagulation. However, the introduction of the parameter δ makes it possible to avoid the minus infinity "catastrophe" in the expression of W at rapid coagulation based on the Fuchs' treatment¹⁴⁾, *vide* the Discussion in the text. In this sense, this treatment is more unified than that derived on the basis of Fuchs' theoretical treatment.

The stability factor, W , is obtained from equation (A. 10) and (A. 12), as

$$W = j^*/j = \frac{\left(1 + \frac{\delta}{\sqrt{\pi \mathcal{D}' t}} \right) (1 + \delta \cdot h)}{\delta \cdot h \{ 1 + \delta \cdot h \exp(h'^2 \mathcal{D}' t) \operatorname{erfc}(h' \sqrt{\mathcal{D}' t}) \}} \quad (\text{A. 14})$$

This equation is rigorous in the sense that no approximation has so far been made. However, it is rather complicated for practical use, so the following assumption will be made:-

$$h' \sqrt{\mathcal{D}' t} > h \sqrt{\mathcal{D}' t} \gg 1$$

$$\text{or} \quad t \gg \mathcal{D}' / (k^0)^2 \quad (\text{A. 15})$$

This means neglect of the transient term, whence

$$W = \frac{1 + \delta \cdot h}{\delta \cdot h} \frac{1 + (\delta / \sqrt{\pi \mathcal{D}' t})}{1 + (\delta / \sqrt{\pi \mathcal{D}' t}) \{ \delta \cdot h / (1 + \delta \cdot h) \}} \quad (\text{A. 16})$$

This equation is consistent, since

for large $\delta \cdot h$, *i. e.* $\delta \cdot h \gg 1$ or $k^0 \gg \mathcal{D}' / \delta$,

$$W = 1 \quad (\text{rapid coagulation})$$

and for small $\delta \cdot h$, *i. e.* $\delta \cdot h \approx 0$ or $k^0 \approx 0$,

$$W = \infty \quad (\text{stable sol}).$$

In the intermediate condition, *i. e.* slow coagulation, a very simple relation is obtained by assuming¹⁵⁾

$$t \gg \delta^2 / \pi \mathcal{D}' \quad (\text{A. 17})$$

Equation (A. 16) reads

$$\begin{aligned} W &= 1 + (1 / \delta \cdot h) \\ &= 1 + (\mathcal{D}' / \delta) (1 / k^0) \end{aligned} \quad (\text{A. 18})$$

because $0 < \delta \cdot h / (1 + \delta \cdot h) < 1/2$.

If we assume $\delta \approx a$ (particle radius), we obtain by the use of equations (5) of Part 1 and (A. 1),

$$W = 1 + (kT / 3 \pi a^2 \eta k_r) \exp(\Delta F^* / kT)$$

$$\text{or} \quad \ln(W - 1) = \ln(kT / 3 \pi a^2 \eta k_r) + (\Delta F^* / kT) \quad (\text{A. 19})$$

REFERENCES

- (1) H. R. Kruyt, "Colloid Science", 2, Elsevier, Amsterdam (1949).
- (2) J. T. Edsall and J. Wyman, "Biophysical Chemistry", 1, Academic Press (1958).
- (3) A. Watanabe, This Bulletin, 38, 179 (1960).
- (4) A. Watanabe, This Bulletin, 38, 158 (1960).
- (5) I. M. Klotz, in Neurath and Baileys', "The Proteins", 1, Academic Press (1953).
- (6) H. Reerink and J. Th. G. Overbeek, *Disc. Faraday Soc.*, 18, 74 (1954).
- (7) A. Watanabe, This Bulletin, Part 5 (1960).
- (8) A. Watanabe, F. Tsuji and S. Ueda, *Proc. 2nd Intern. Congr. Surface Activity, London*, 3, 94 (1957); this Bulletin, 33, 91 (1955); 34, 1, 65 (1955).
- (9) D. C. Grahame, *Chem. Rev.*, 41, 441 (1947).
- (10) E. A. Guggenheim, *J. phys. Chem.*, 33, 842 (1929).
- (11) S. Glasstone, K. Laidler and H. Eyring, "The Theory of Rate Processes", McGraw Hill, New York (1941).
- (12) P. Delahay, "New Instrumental Methods in Electrochemistry", Interscience, New York (1954).
- (13) F. C. Collins and G. E. Kimball, *J. Colloid Sci.*, 4, 425 (1949).
- (14) N. Fuchs, *Z. Physik*, 89, 736 (1934).
- (15) H. R. Kruyt, "Colloid Science", 1, Elsevier, Amsterdam (1948).